Electrochimica Acta 94 (2013) 320–326

Contents lists available at SciVerse ScienceDirect

Electrochimica Acta

journal homepage: www.elsevier.com/locate/electacta

Variation in the iron oxidation states of magnetite nanocrystals as a function of crystallite size: The impact on electrochemical capacity

Melissa C. Menard[a,b], Amy C. Marschilok[a,b,*], Kenneth J. Takeuchi[a,*], Esther S. Takeuchi[a,b,c,*]

[a] Department of Chemistry, Stony Brook University (SUNY), Stony Brook, NY 11794, USA
[b] Department Materials Science and Engineering, Stony Brook University (SUNY), Stony Brook, NY 11794, USA
[c] Global and Regional Solutions Directorate, Brookhaven National Laboratory, Upton, NY 11973, USA

ARTICLE INFO

Article history:
Received 31 December 2012
Received in revised form 29 January 2013
Accepted 1 February 2013
Available online 9 February 2013

Keywords:
Magnetite
Crystallite size
Rietveld
X-ray absorption spectroscopy
X-ray absorption near edge structure

ABSTRACT

We have investigated magnetite (Fe_3O_4) as an electroactive battery electrode material, where a linear relationship was observed between Fe_3O_4 crystallite size and capacity, with a negative slope. In order to better understand this novel relationship, we report here the Rietveld refinement and X-ray absorption spectroscopy (XAS) investigation of nanosized Fe_3O_4 as a function of crystallite size (7–26 nm). Rietveld refinement established that the Fe_3O_4 samples were phase pure, while the extended X-ray absorption fine structure (EXAFS) and X-ray absorption near edge structure (XANES) provided insight into the local geometries and electronic structure of the iron centers, including oxidation state assignment. From our current and recent studies, we suggest that the surface of the Fe_3O_4 crystallites is rich in Fe^{3+}, thus as the Fe_3O_4 crystallite size decreases, the electrochemical capacity increases, due to a net enrichment of Fe_3O_4 in Fe^{3+}.

1. Introduction

Nanostructured materials possess important properties which can affect the electrochemistry of Li-ion batteries. For example, reducing crystallite dimension can decrease the path length for the transport of ions and electrons, which has been linked to higher achieved capacity of electrode materials in particular under high rate discharge [1–7]. In addition to reducing the path length for charge transport, additional advantages associated with battery electrodes containing nanostructured materials include better accommodation of the structural strain associated with lithium insertion/removal and increased electrode/electrolyte contact area contributing to improved rate capability [1,8,9].

Magnetite (Fe_3O_4) has been the subject of a variety of studies, including electrochemistry studies of Fe_3O_4 as a possible battery electrode material [4,10–15]. Specifically, the effects of crystal dimension on the electrochemistry of nanostructured Fe_3O_4 are the subject of several recent reports. For example, a critical aspect of our research involving the electrochemistry of Fe_3O_4 is our ability to control and vary the crystallite size of Fe_3O_4 by direct synthetic methods without using constraining media. We reported magnetite-based cathodes (~6–10 nm) with a 30% increase in delivered capacity attributed to decreasing crystallite size across the series [16,17]. Komaba et al investigated the Fe_3O_4 crystallite size effect in rechargeable lithium batteries, where their 10 nm sample delivered 130 mAh/g, while the 400 nm sample delivered only 7 mAh/g when discharged to 1.5 V [11]. In a follow up study, they reported 190 mAh/g of rechargeable capacity in the 2–3 V range for the 10 nm sample, while the 400 nm and 100 nm Fe_3O_4 showed significantly lower capacities of 10 and 80 mAh/g respectively [18]. Additional recent reports indicate reasonable cycling and rate performance for nanostructured Fe_3O_4 [3–6,19–21]. In order to better understand the pronounced effect of Fe_3O_4 crystallite size on delivered capacity, the structural changes accompanying varying Fe_3O_4 crystallite size deserve further inspection.

We report here the Rietveld refinement, X-ray absorption spectroscopy (XAS) and electrochemical assessment of Fe_3O_4 as a function of crystallite size. The Rietveld refinement of Fe_3O_4 nanocrystals provides bulk structural information, while extended X-ray absorption fine structure (EXAFS) and X-ray absorption near edge structure (XANES) of Fe_3O_4 nanocrystals provide details concerning local geometries and electronic structure of the iron centers, including oxidation state assignment. Notably, we observed a variation in the average oxidation state of the iron centers in Fe_3O_4 as a function of crystallite size, where smaller crystallites of Fe_3O_4 display an increase in average oxidation state of the

* Corresponding authors at: Department of Chemistry, Stony Brook University (SUNY), Stony Brook, NY 11794-3400, USA. Tel.:+1 16316327880.
E-mail addresses: amy.marschilok@stonybrook.edu (A.C. Marschilok), kenneth.takeuchi.1@stonybrook.edu (K.J. Takeuchi), esther.takeuchi@stonybrook.edu (E.S. Takeuchi).

0013-4686/$ – see front matter © 2013 Elsevier Ltd. All rights reserved.
http://dx.doi.org/10.1016/j.electacta.2013.02.012

iron centers. This increase in iron oxidation states associated with a decrease in Fe_3O_4 nanocrystal size could provide profound insight into the electrochemical capacity enhancement associated with a decrease in Fe_3O_4 nanocrystal size.

2. Experimental

Formation of Fe_3O_4 in various crystallite sizes was accomplished by using aqueous solutions of iron(III) chloride hexahydrate, iron(II) chloride tetrahydrate, and triethylamine which were combined as previously described [16,17]. Product was isolated from the aqueous solution and then dried *in vacuo*. Commercially obtained samples of FeO, Fe_3O_4, α-Fe_2O_3 purchased from Alfa AESAR were used as reference materials for X-ray absorption spectroscopy (XAS) analysis. Commercially obtained samples of Fe_2O_3 and FeO were also physically mixed in several mass ratios (25:75, 50:50, and 75:25), and used as additional reference materials for XAS analysis.

The products were identified by X-ray powder diffraction (XRD) using a Rigaku Ultima-IV diffractometer with Cu Kα radiation as magnetite, Fe_3O_4 (PDF no. 00-019-0629) [22]. The XRD data were measured in a 2θ range from 5 to 90° with a step width of 0.05° and a scan rate of 1°/min. Structure refinement of samples were performed using the GSAS software package and the EXPGUI interface [23,24]. The profiles were fit using Thompson–Cox–Hastings pseudo-Voigt profile function and the background was fit using a shifted Chebyshev polynomial with 8 terms [25,26]. Peak tails were ignored where the intensity was below 0.030 times the peak. The isotropic crystallite sizes, or average crystal dimensions, were extracted from the Rietveld refinement [27,26].

Fe K-edge X-ray absorption spectra were collected at room temperature in transmission mode on station X-11B of the National Synchrotron Light Source at Brookhaven National Laboratory with the electron storage ring operating at 2.8 GeV and a stored current in the range of 200–300 mA [28]. The Fe K-edge was extracted from the white radiation using a Si (1 1 1) double crystal monochromator, and the incident and transmitted beams were monitored using ionization chambers with flowing nitrogen and argon. Two scans of each sample were collected and merged.

XAS data were analyzed using the Athena software package [29]. All spectra were calibrated and aligned using foil scans collected simultaneously with each sample followed by normalization to obtain an edge jump of unity. EXAFS modeling was carried out using the Artemis software package to obtain bond distances corresponding to the first and second shells of magnetite [29]. FEFF6 calculations were used to determine all the scattering paths in a cluster of ~9 atoms out to a distance of 6 Å from the photoabsorbing Fe atom using single crystal data for Fe_3O_4 [22]. A k-range of 3.2–15 $Å^{-1}$ and the Fourier transform (FT) range of 1.0–3.6 Å were set for Fe K-edge data using Hanning window. The scattering amplitude Amp, scaled according to the multiplicity of each Fe site, the energy shift ΔE_0, the Debye–Waller factor σ^2, and a single scattering path shift ΔR were used in EXAFS fitting for all paths.

Experimental 2-electrode cells were fabricated as previously described in an inert atmosphere glove box using lithium metal anodes and Fe_3O_4 cathodes [16,17]. The cells were tested at 30 °C under constant current discharge with a current density of 2.3×10^{-5} A cm^{-2}.

3. Results and discussion

3.1. Structural characterization by Rietveld refinement

The magnetite structure (Fig. 1) is traditionally described as a cubic close-packed array of oxide ions with Fe^{3+} ions in the tetrahedral interstices and both Fe^{2+} and Fe^{3+} ions occupying the

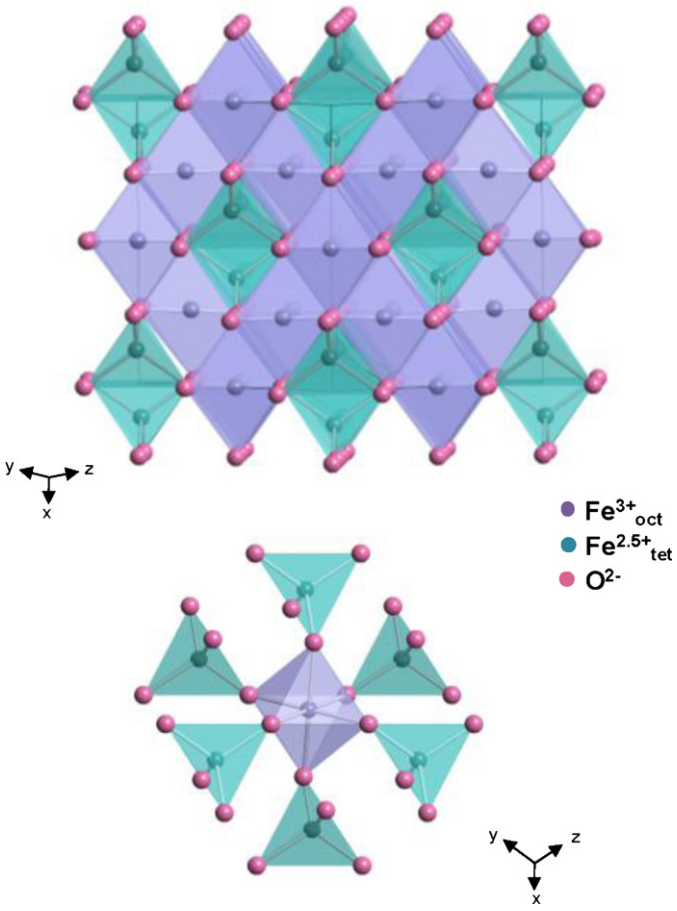

Fig. 1. Crystallographic structure of Fe_3O_4.

octahedral interstices, equally [30]. The $[Fe^{+2.5}{}_2O_4]$ component is a derivative of the rock-salt structure containing a cubic closed packed array of oxide ions with alternate octahedral sites occupied equally by Fe^{2+} and Fe^{3+}. In order to minimize cation–cation repulsions and simultaneously satisfy electroneutrality, the remaining Fe^{3+} ions occupy tetrahedral sites for which all neighboring octahedral sites are empty.

Our unique synthesis of magnetite nanoparticles, a low-temperature coprecipitation method, allowed the systematic variation of crystallite size with reactant concentration, in the absence of a constraining medium [16]. We report here peak broadening due to decreasing crystallite size and low crystallinity which can be seen on examination of the 3 1 1-peak when the XRD patterns are overlaid (Fig. 2).

As the crystallite size can be significantly reduced via the coprecipitation method, we wished to verify that the material prepared at all crystallite sizes was consistent with an inverse-spinel Fe_3O_4 crystallographic structure. Here we report the Rietveld refinement of Fe_3O_4 of a range of samples including commercially obtained bulk materials (>200 nm), commercially obtained large crystallite size material (26.2 nm), and our smaller crystallite size materials prepared by coprecipitation (8.4–10.9 nm). Crystallographic parameters, atomic positions, and interatomic distances resulting from the refinement are summarized below (Tables 1–3). Refinement plots showing comparison of observed and calculated data are provided for the 26.2, 10.9, and 8.4 nm samples (Fig. 3). Rietveld refinement showed all samples maintained the average cubic inverse-spinel structure. There are no notable trends in bond lengths as a function of crystallite size (Table 3). There are no notable trends in bond angles as a function of crystallite